Faculty of Geodesy and Cartography
Warsaw University of Technology

Open-Source vs. Commercial Photogrammetry: Comparing Accuracy and Efficiency of OpenDroneMap and Agisoft Metashape

Adam Kostrzewa, Anna Płatek-Żak, Przemysław Banat, Łukasz Wilk

EuroCOW - EUROPEAN WORKSHOP ON CALIBRATION AND ORIENTATION IN REMOTE SENSING
16.06.2025

Presentation agenda

1. Background & aim of the study

Provides context and purpose for the study.

2. Technical overview

Introduces the software used in the study.

3. Study area & datasets

Describes the location and data used.

4. Methods

Outlines the procedures followed in the study.

5. Results & conclusions

Presents the findings and their implications.

1. Background & aim of the study

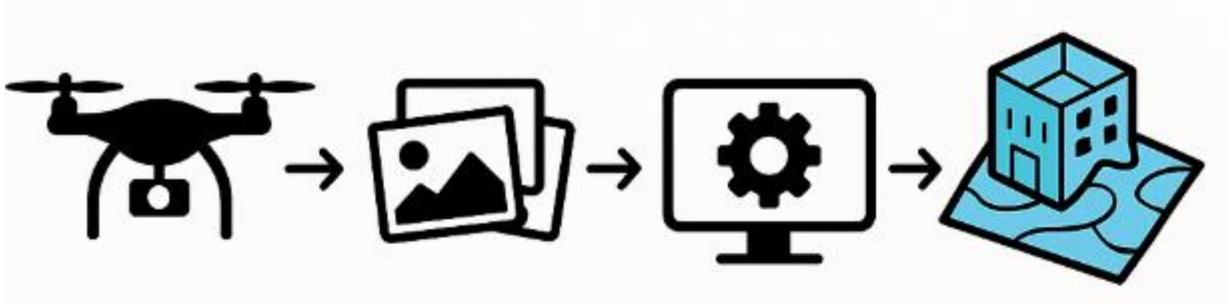

Who needs photogrammetry?

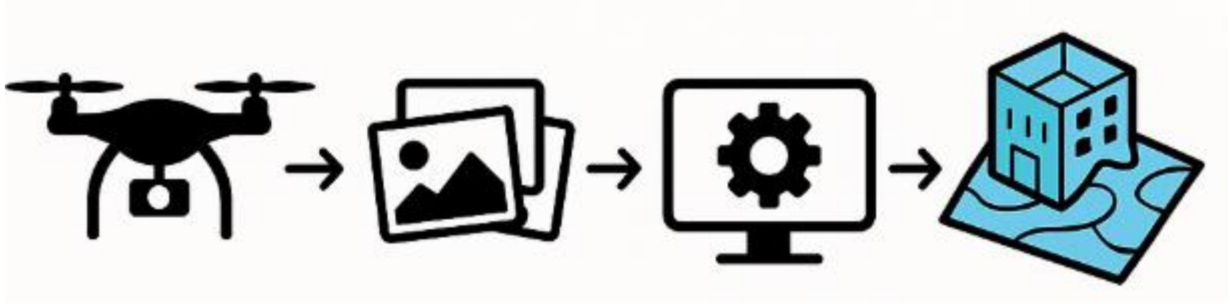

Who needs photogrammetry?

Photogrammetry is everywhere - but not everyone can afford it

Cost Comparison of the most popular solutions

Agisoft Metashape
Professional Edition

Node-locked license

$ 3 499

PIX4Dmapper

Perpetual

€4,690 / one-time

Billed one time, excl. taxes

Is there a more affordable option?

Background & Aim of the Study

Can free software be as good as commercial solutions?

OpenDroneMap™

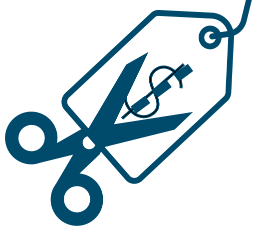

Comparison of OpenDroneMap and Agisoft Metashape

Does expensive mean better?

Why Compare?

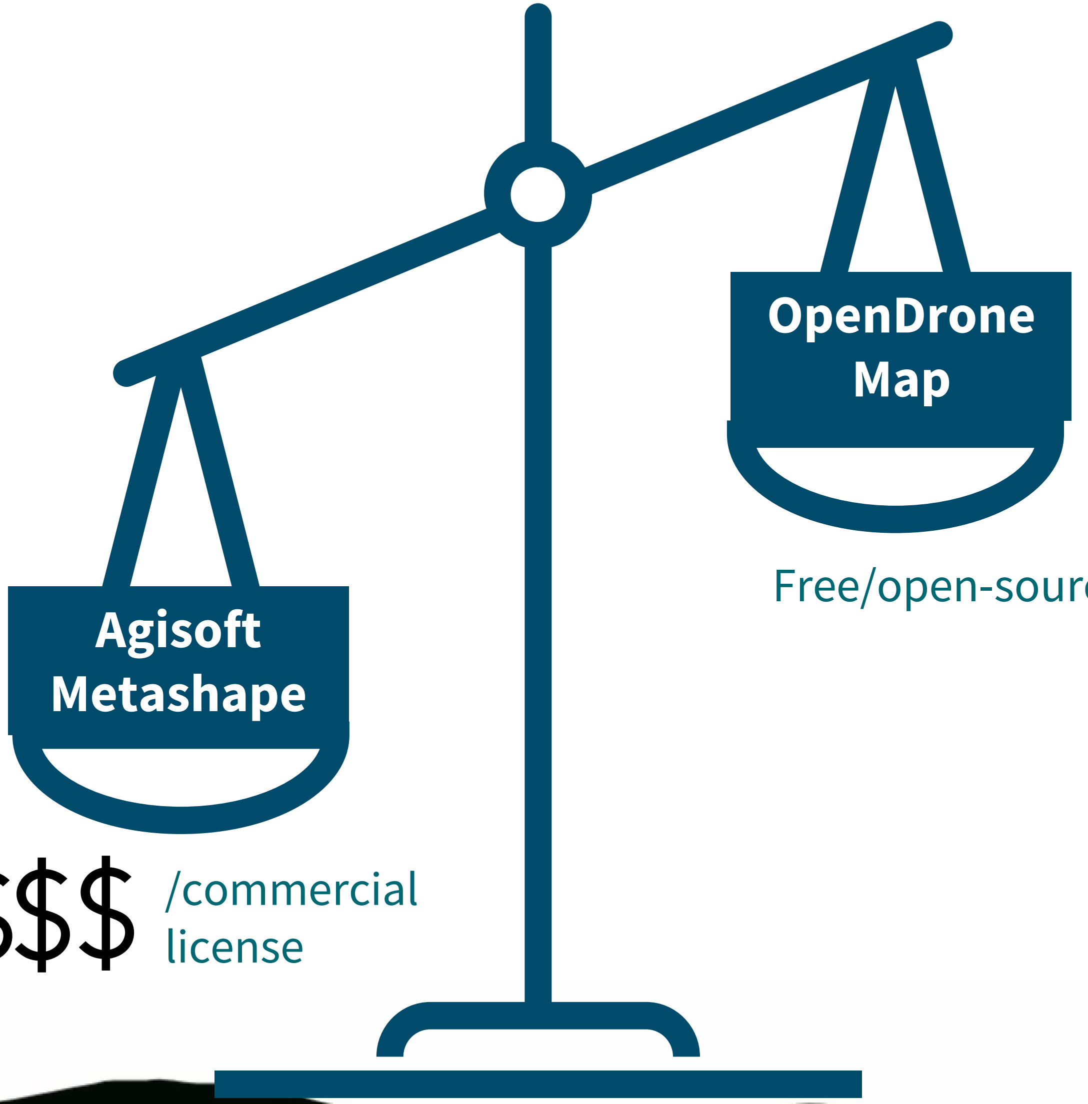

Free/open-source

$$$ /commercial license

2. Technical overview

Comparison of OpenDroneMap and Agisoft Metashape

Metashape Professional

- GCPs, ChPs
- GUI
- Python API
- MSI, thermal LiDAR data processing
- GPU (CUDA and OpenCL)
- Built-in SfM/MVS

OpenDroneMap

- PoissonRecon
- Only GCPs
- CLI/GUI
- SMPF Point Cloud
- limited MSI processing
- no GPU required
- openSFM, open MVS

3. Study area & datasets

Study area and datasets

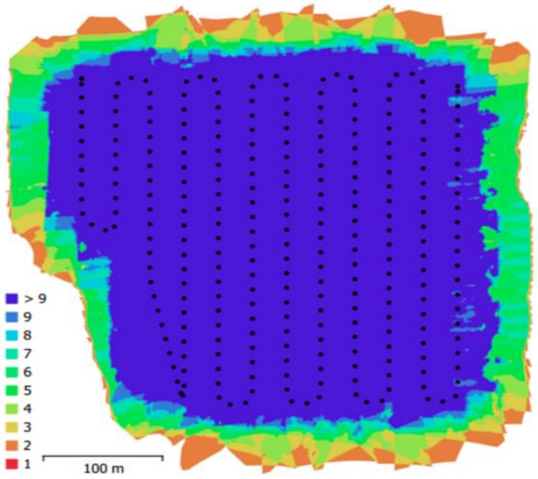

Józefosław

No. of scenario	1a
Dataset name	**JOZE**
Image type	RGB, nadir
UAV platform	DJI Mavic 3 Multispectral
Camera model	DJI M3M
GCPs and ChPs	-
Focal length [mm]	12.29
Pixel size [µm]	3.36
Image resolution	5280 x 3956
Field of view [°]	84
Image overlap [%]	85/75
Survey area [km^2]	0.024
Number of strips	12
Flying altitude [m]	87
GSD [cm]	2.2
Number of images	266
Gimbal pitch angle [°]	0

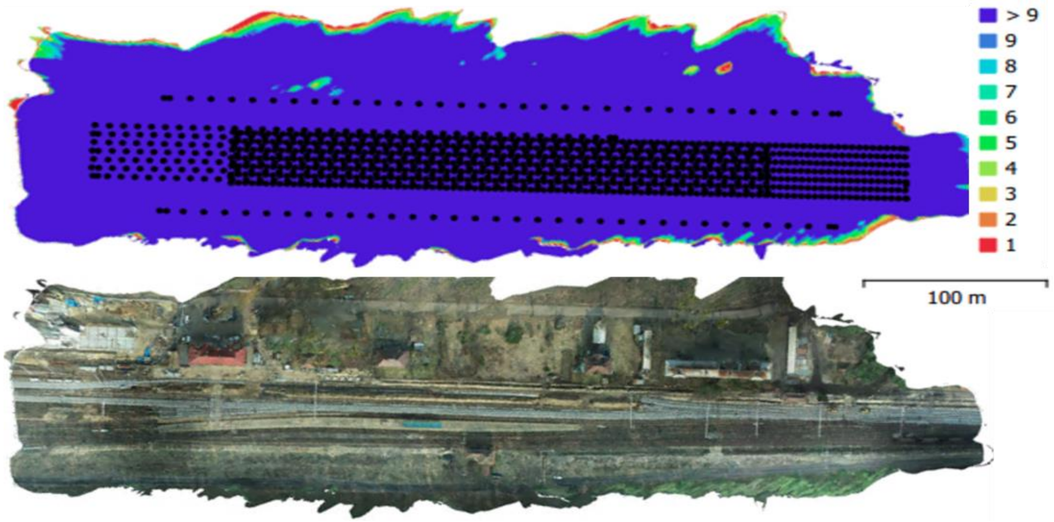

Scenarios 1b and 2b

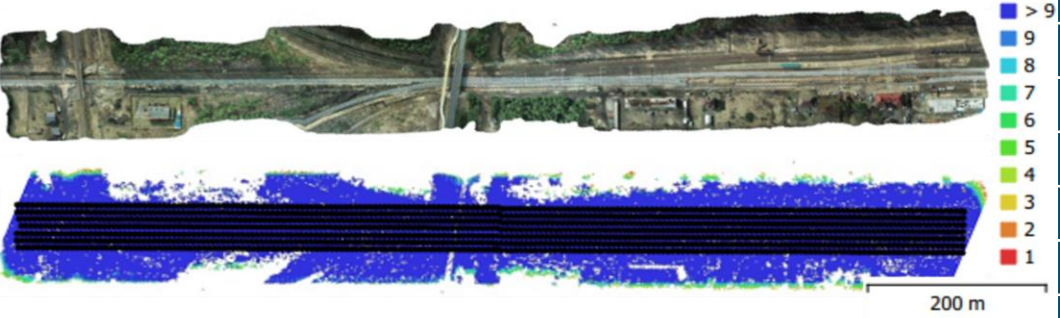

Scenario 2a

Herby

No. of scenario	1b	2a	2b
Dataset name	Herby		
Image type	RGB, oblique	RGB, nadir	RGB, oblique
UAV platform	DJI Phantom 4 RTK		
Camera model	DJI FC6310R		
GCPs and ChPs	-	57 ChPs, 7 ChPs	29 ChPs, 5 GCPs
Focal length [mm]	8.8		
Pixel size [μm]	2.41		
Image resolution	5472 x 3648		
Field of view [°]	84		
Image overlap [%]	90/90	90/90	90/90
Survey area [km^2]	0.071	0.117	0.071
Number of strips	16	7	16
Flying altitude [m]	46	56	46
GSD [cm]	1.2	1.5	1.2
Number of images	1102	1358	1102
Gimbal pitch angle [°]	45	0	45

Study area and datasets

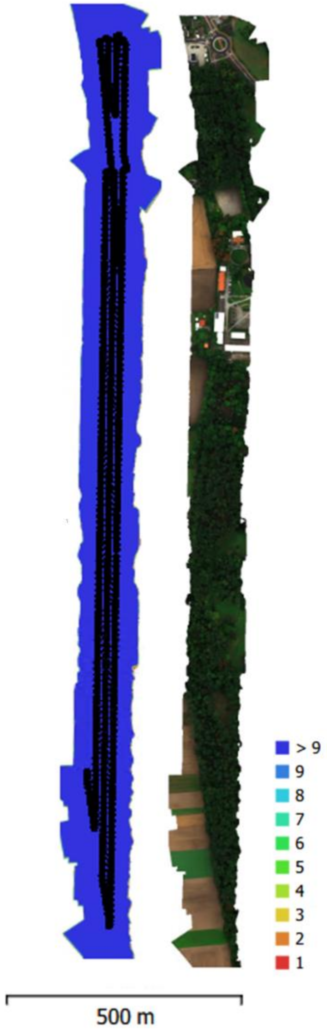

Gołuchów

No. of scenario	**3**
Dataset name	**Gołuchów**
Image type	MSI, nadir
UAV platform	DJI Matrice 300 RTK
Camera model	Micasense RedEdge-MX Dual
GCPs and ChPs	-
Focal length [mm]	5.5
Pixel size [µm]	3.75
Image resolution	1280 x 960
Field of view [°]	47.2
Image overlap [%]	80/80
Survey area [km^2]	0.268
Number of strips	3
Flying altitude [m]	85
GSD [cm]	6.3
Number of images	500
Gimbal pitch angle [°]	0

4. Methods

Methods

Setup Scenarios

Establishing different research scenarios for testing

Compare Software Performance

Comparing the performance of ODM and Metashape

Test Orientation Quality

Evaluating the quality of image orientation

Analyze Calibration Accuracy

Analyzing the accuracy of calibration parameters

Test Camera Calibration

Assessing the accuracy of camera calibration

Visualize Distortions

Visualizing radial and tangential distortions

Scenario 1: Orientation & Calibration (No GCPs)

- 1a: RGB Nadir Imagery, Varied Pyramid Levels
- 1b: RGB Oblique Imagery, Varied Pyramid Levels

Scenario 2: Orientation & Calibration (With GCPs)

- 2a: RGB Nadir Imagery at Original Resolution
- 2b: RGB Oblique Imagery at Original Resolution

Scenario 3: Multispectral Image (MSI) Processing

- Overview of MSI Data Processing
- Calibration and Orientation of MSI Data

5. Results & conclusions

Results: Scenario 1a

The results obtained for processing scenario 1a, the JOZE dataset in the ODM software.

Level	Lowest	Low	Medium	High	Ultra
GPS error [m]	0.003	0.011	0.033	0.052	0.055
Avg. Rep Error [pix]	2.03	1.78	1.37	1.12	1.13
Focal [mm]	11.6947	11.8934	12.3245	12.4860	12.4842
Cx [µm]	8.87	7.10	7.10	8.87	8.70
Cy [µm]	-90.39	-89.06	-83.74	-81.08	-79.75
P1	-0.0001	-0.0001	-0.0001	-0.0004	-0.0004
P2	-0.0005	-0.0005	-0.0004	-0.0001	-0.0001
K1	-0.0818	-0.0928	-0.1053	-0.1094	-0.1093
K2	-0.0243	-0.0120	0.0022	0.0061	0.0062
K3	0.0028	-0.0029	-0.0167	-0.0213	-0.0216

The results obtained for processing scenario 1a, the JOZE dataset in the Metashape software.

Level	Lowest	Low	Medium	High	Highest
GPS error [m]	0.218	0.122	0.150	0.112	0.076
Avg. Rep Error [pix]	7.12	3.32	1.50	1.17	0.95
Focal [mm]	13.7726	13.0379	13.4805	13.3928	13.2718
Cx [µm]	5.36	12.92	13.06	13.63	12.10
Cy [µm]	-77.33	-102.75	-90.32	-87.96	-90.68
P1	-0.0004	-0.0004	-0.0004	-0.0004	-0.0004
P2	-0.0004	-0.0002	-0.0002	-0.0003	-0.0003
K1	-0.1303	-0.1194	-0.1292	-0.1272	-0.1250
K2	-0.0024	-0.0087	0.0158	0.0129	0.0119
K3	-0.0240	-0.0288	-0.0410	-0.0367	-0.0343

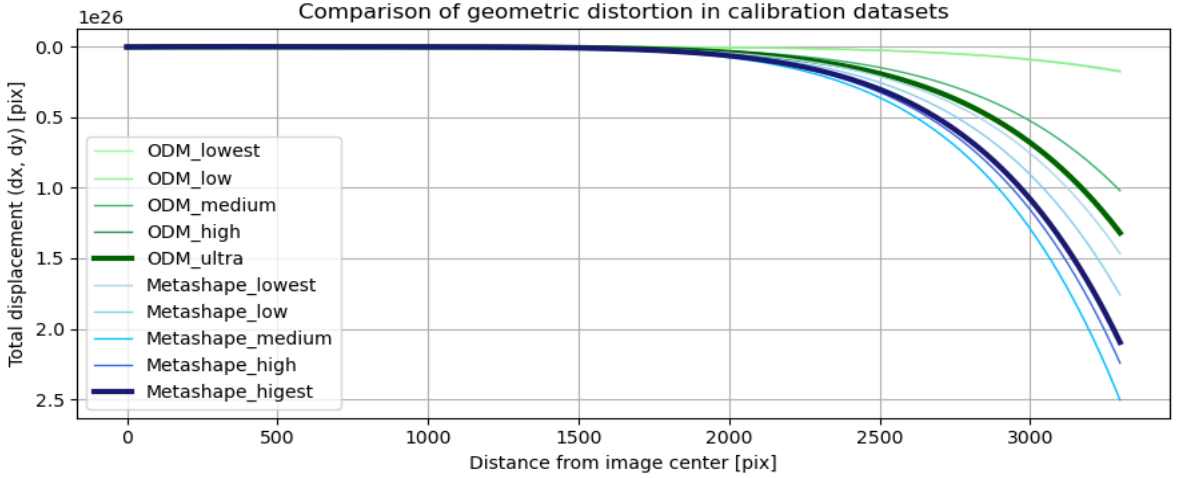

Results: Scenario 1b

The results obtained for processing scenario 1b, the Herby Oblique dataset in the ODM software.

Level	Lowest	Low	Medium	High	Ultra
GPS error [m]	0.001	0.013	0.27	0.038	0.037
Avg. Rep Error [pix]	2.12	1.81	1.41	1.15	1.16
Focal [mm]	8.9003	8.9108	8.9108	8.9095	8.9082
Cx [µm]	-13.2	-43.5	-54.1	-63.3	-64.6
Cy [µm]	12.3	5.3	6.2	6.2	7.9
P1	0.0000	-0.0003	-0.0001	-0.0001	-0.0001
P2	-0.0003	-0.0011	-0.0013	-0.0013	-0.0013
K1	-0.0122	-0.0134	-0.0142	-0.0136	-0.0134
K2	0.0003	0.0003	0.0014	0.0001	-0.0005
K3	0.0051	0.0082	0.0079	0.0088	0.0094

The results obtained for processing scenario 1b, the Herby Oblique dataset in the Metashape software.

Level	Lowest	Low	Medium	High	Highest
GPS error [m]	0.002	0.006	0.008	0.010	0.011
Avg. Rep Error [pix]	5.66	2.52	1.54	0.97	0.77
Focal [mm]	8.8923	8.8963	8.9003	8.9011	8.8992
Cx [µm]	-47.60	-44.12	-44.95	-44.77	-45.19
Cy [µm]	29.35	27.30	23.57	21.80	22.35
P1	-0.0015	-0.0015	-0.0015	-0.0015	-0.0015
P2	-0.0002	-0.0001	-0.0001	-0.0001	-0.0001
K1	-0.0128	-0.0142	-0.0132	-0.0129	-0.0119
K2	-0.0020	0.0014	-0.0008	-0.0013	-0.0045
K3	0.0107	0.0080	0.0098	0.0099	0.0126

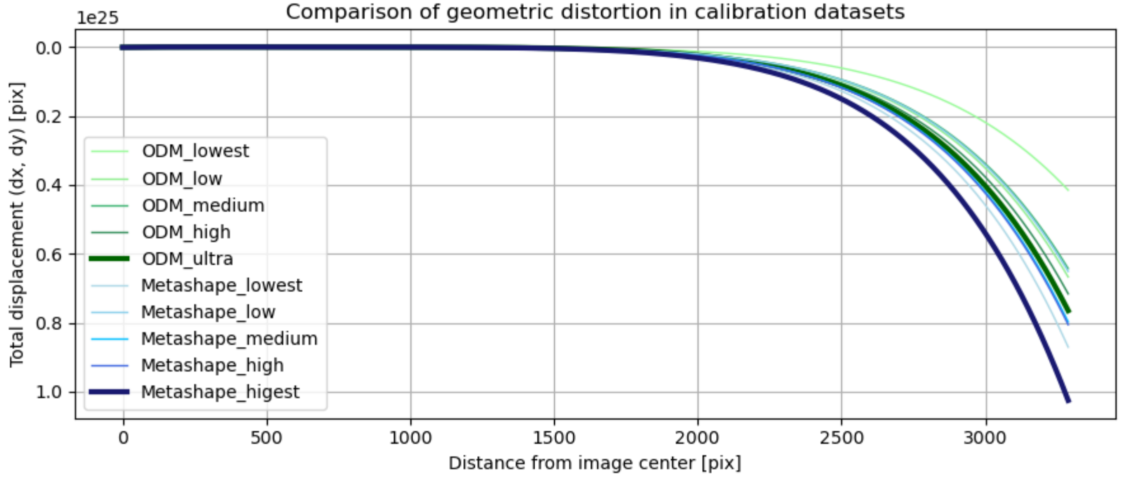

Results: Scenario 2

The results obtained for processing scenario 2a the Herby Nadir dataset with GCPs

Software & Settings	ODM (ultra)	Metashape (highest)
Total RMS GCPs [m]	0.001	0.040
Avg. Rep Error [pix]	1.19	0.61
Focal [mm]	9.1970	8.9134
Cx [µm]	5.28	-39.46
Cy [µm]	38.68	23.17
P1	-0.0001	-0.0015
P2	-0.0016	-0.0001
K1	-0.0143	-0.0157
K2	-0.0001	-0.0016
K3	0.0104	0.0099

The results obtained for processing scenario 2b the Herby Oblique dataset with GCPs

Software & Settings	ODM (ultra)	Metashape (highest)
Total RMS GCPs [m]	0.006	0.029
Avg. Rep Error [pix]	1.18	0.77
Focal [mm]	8.9121	8.8998
Cx [µm]	-54.07	-45.02
Cy [µm]	7.03	23.85
P1	-0.0001	-0.0015
P2	-0.0013	-0.0001
K1	-0.0134	-0.0118
K2	-0.0007	-0.0045
K3	0.0098	0.0126

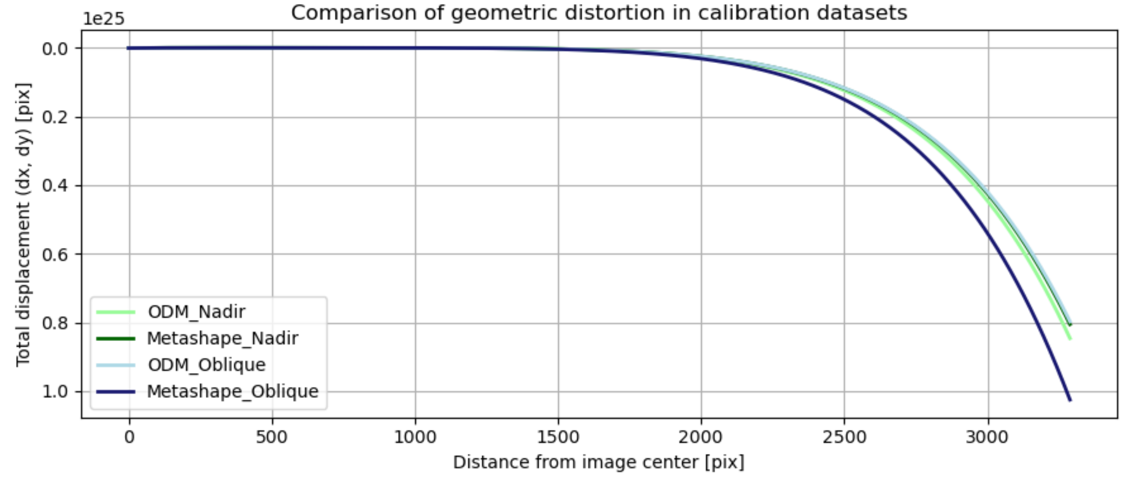

Results: Scenario 2

The results obtained for processing scenarios 2a and 2b on GCPs.

Software & Image type	RMSE GCPs [m]			
	X	Y	Z	Total
ODM nadir	0.001	0.000	0.001	0.001
Metashape nadir	0.025	0.026	0.018	0.040
ODM oblique	0.002	0.010	0.004	0.006
Metashape oblique	0.015	0.009	0.023	0.029

The results obtained for processing scenarios 2a and 2b on Check Points.

Software & Image type	RMSE Check Points [m]			
	X	Y	Z	Total
ODM nadir	0.032	0.044	0.038	0.067
Metashape nadir	0.022	0.016	0.026	0.038
ODM oblique	0.045	0.063	0.036	0.085
Metashape oblique	0.018	0.010	0.026	0.033

Results: Multispectral imagery processing

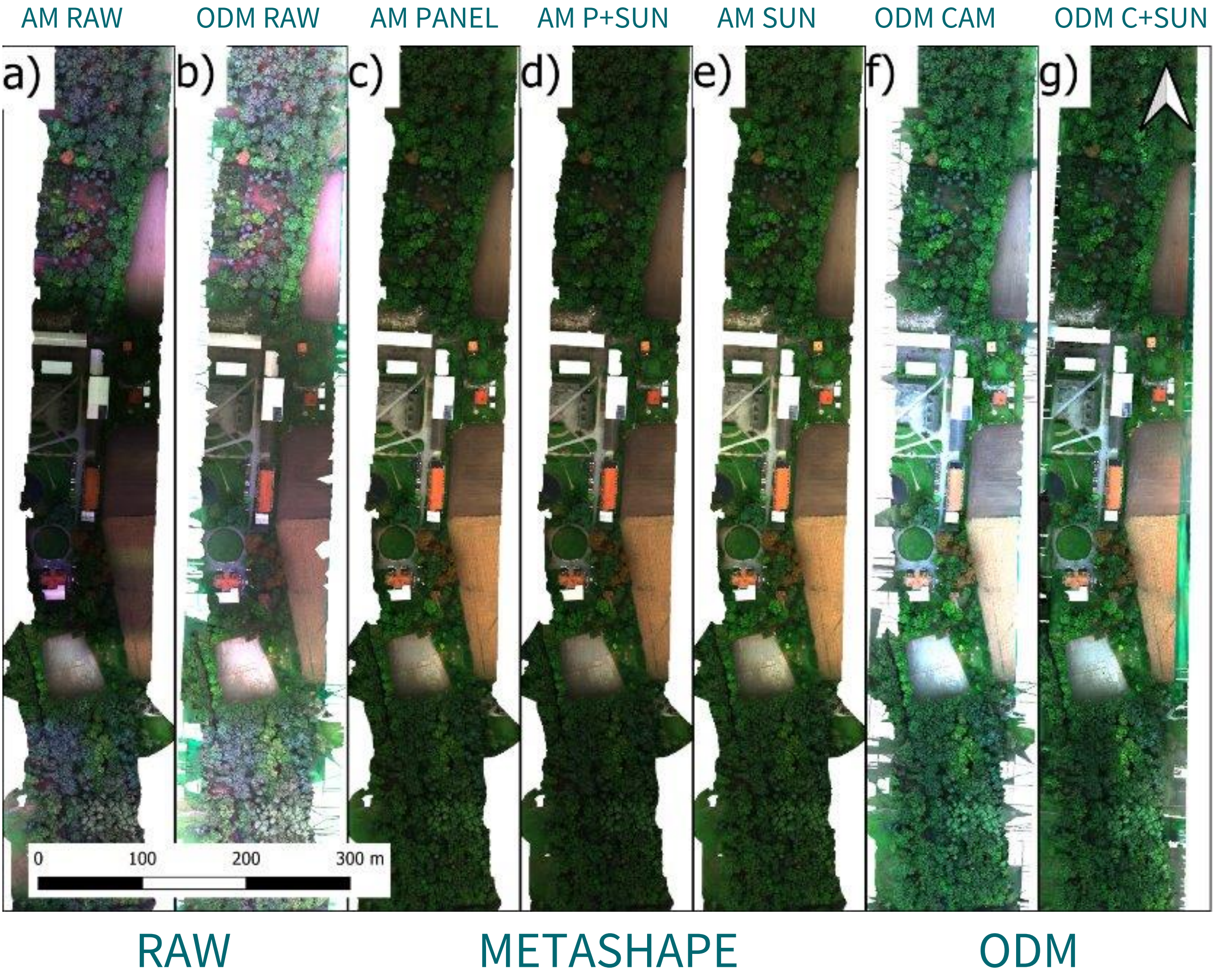

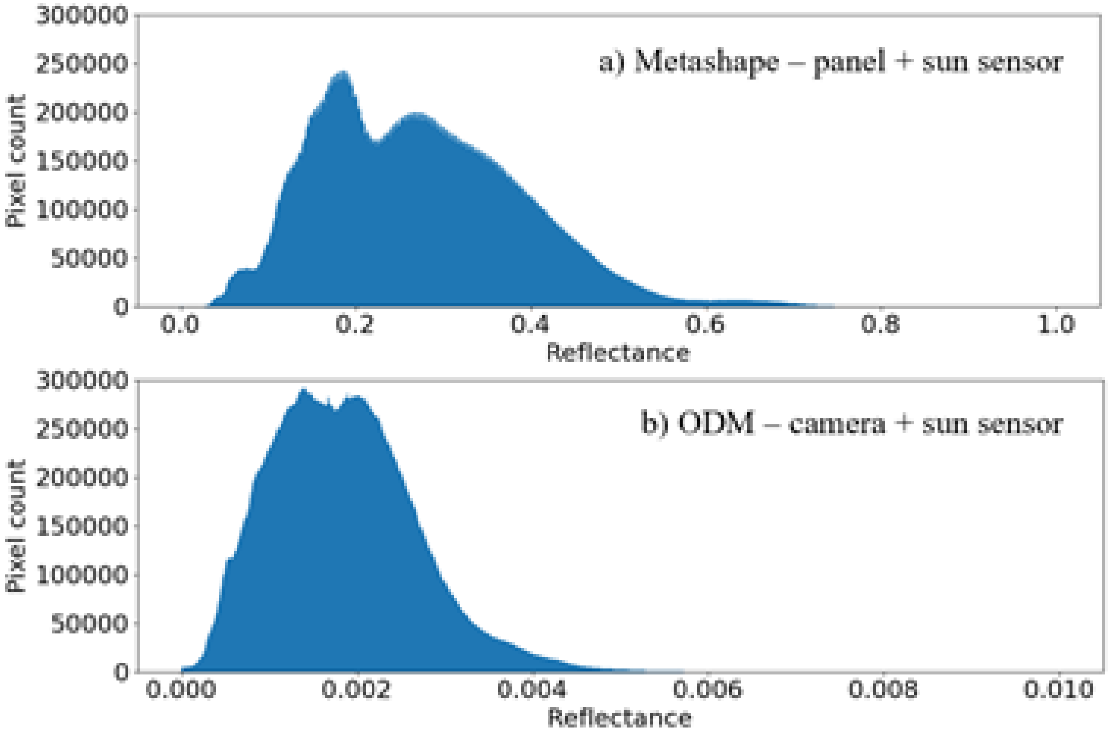

ODMs ability to perform radiometric calibration is limited to correction of exposure changes and use of sun sensor data without reference panels. In practice, the radiometric values are consistent within the mosaic, but the absolute values of reflectance are questionable.

Conclusions

Comparable Calibration Results

Limited Georeferencing

Basic MSI Processing

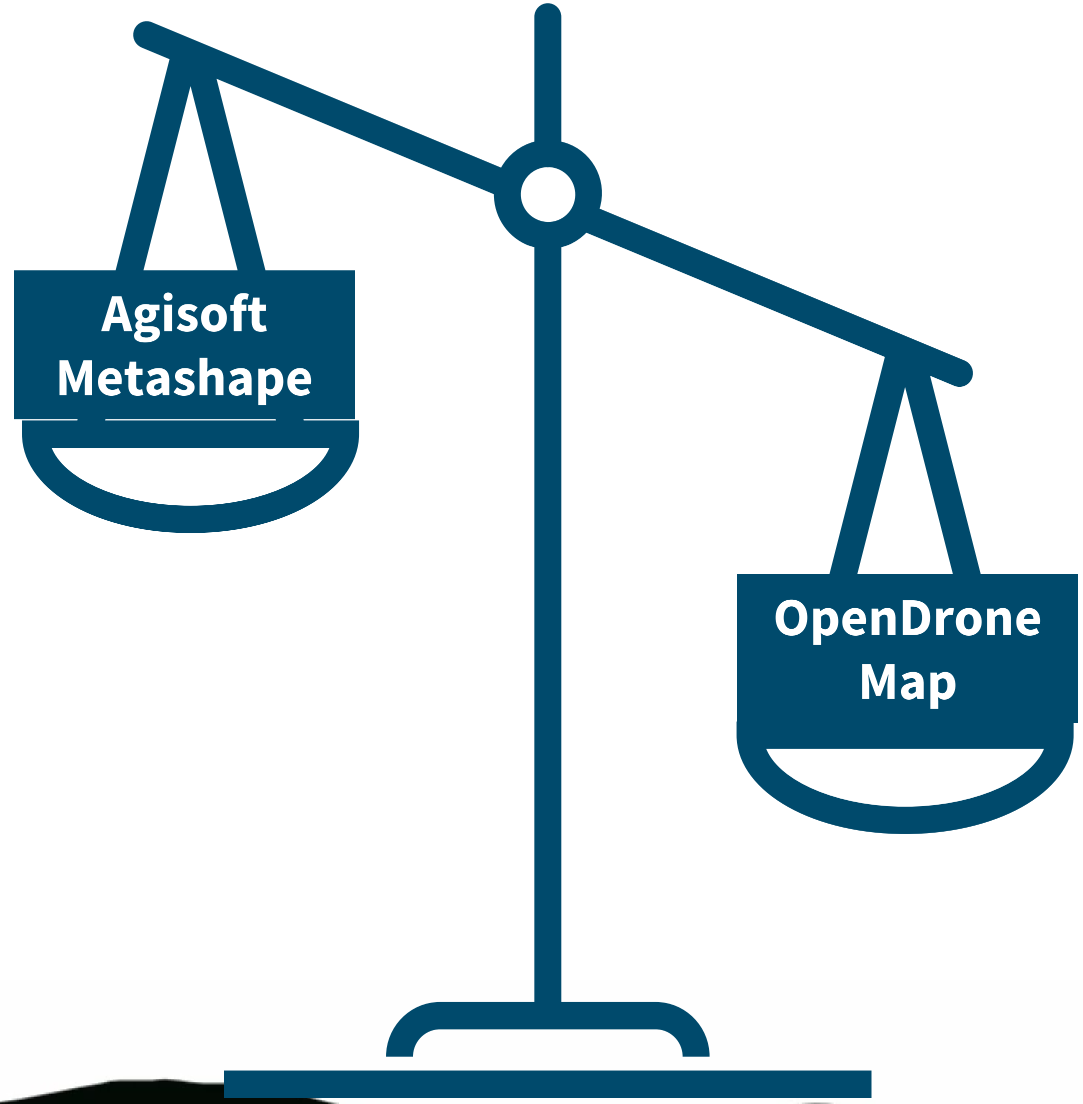

Advanced Calibration Tools

Robust Georeferencing

Comprehensive MSI Processing

References

Agisoft LLC. (2025). Agisoft Metashape user manual: Professional Edition (Version 2.2). Agisoft LLC.

Burdziakowski, P. (2017). Evaluation of open drone map toolkit for geodetic grade aerial drone mapping – case study. International Multidisciplinary Scientific GeoConference Surveying Geology and Mining Ecology Management, SGEM, 17(23), 101-110.

DJI, 2025a: Phantom 4 RTK Technical Data, https://www.dji.com/de/phantom-4-rtk/info. Access:14.05.2025

DJI, 2025b: Phantom 4 RTK Technical Data, https://dji.com/pl/support/product/matrice-300. Access:14.05.2025

DJI, 2025c: Phantom 4 RTK Technical Data, https://ag.dji.com/mavic-3-m/specs. Access: 14.05.2025

Fryskowska-Skibniewska, A., Kedzierski, M., Sekrecka, A., Braula, A., (2016). Calibration of low cost RGB and NIR UAV cameras. ISPRS - International Archives of the Photogrammetry, Remote Sensing and Spatial Information Sciences. XLI-B1. 817-821.

Garcia, Y., de Oliveira, H. C., Fernandes, R., Costa, D., (2020). Evaluation of Different Methods for Non-Metric Camera Calibration. Anuario do Instituto de Geociencias. 43. 266-272.

Gbagir, A. M. G., Ek, K., & Colpaert, A. (2023). OpenDroneMap: multi-platform performance analysis. Geographies, 3(3), 446-458.

Groos, A. R., Bertschinger, T. J., Kummer, C. M., Erlwein, S., Munz, L., & Philipp, A. (2019). The potential of low-cost UAVs and open-source photogrammetry software for high-resolution monitoring of Alpine glaciers: a case study from the Kanderfirn (Swiss Alps). Geosciences, 9(8), 356.

Jełowicki, Ł., Sosnowicz, K., Ostrowski, W., Osińska-Skotak, K., & Bakuła, K. (2020). Evaluation of rapeseed winter crop damage using UAV-based multispectral imagery. Remote Sensing, 12(16), 2618.

Kaimaris, D., Patias, P., & Sifnaiou, M. (2017). UAV and the comparison of image processing software. International Journal of Intelligent Unmanned Systems, 5(1), 18-27.

Kloc, B., Mazur, A., & Szumiło, M. (2021). Comparison of free and commercial software in the processing of data obtained from non-metric cameras. Journal of Ecological Engineering, 22(2).

Martinez Batlle, J. (2018). Digital photogrammetry of historical aerial photographs using open-source software. EarthArXiv eprints, BNA95.

Mora-Félix, Z. D., Rangel-Peraza, J., Monjardin, S. & Sanhouse-García, A. (2024). Performance and precision analysis of 3D surface modeling through UAVs: validation and comparison of different photogrammetric data processing software. Physica Scripta. 99.

Näsi, R., Honkavaara, E., Blomqvist, M., Lyytikäinen-Saarenmaa, P., Hakala, T., Viljanen, N., ... & Holopainen, M. (2018). Remote sensing of bark beetle damage in urban forests at individual tree level using a novel hyperspectral camera from UAV and aircraft. Urban Forestry & Urban Greening, 30, 72-83.

Nikolakopoulos, K. & Koukouvelas, J. (2017). Commercial vs professional UAVs for mapping. Fifth International Conference on Remote Sensing and Geoinformation of the Environment, 1044409 (6 September 2017),

ODM. (2021). Feature Request: Additional Control Point Types #1302. https://github.com/OpenDroneMap/ODM/issues/1302

OpenDroneMap Authors. (2020). ODM - A command line toolkit to generate maps, point clouds, 3D models and DEMs from drone, balloon or kite images. OpenDroneMap/ODM GitHub Page. https://github.com/OpenDroneMap/ODM OpenDroneMap GitHub repository, (2022) https://github.com/OpenDroneMap/ODM/blob/master/opendm/multispectral.py

Ostrowski, W. & Bakuła, K., (2016). Towards efficiency of oblique images orientation. ISPRS - International Archives of the Photogrammetry, Remote Sensing and Spatial Information Sciences. XL-3/W4. 91-96.

Ostrowski, W., Miszk, Ł., Modrzewski, J., Wilk, Ł., & Lech, P. (2024). Monitoring of large-scale archaeological excavations using photogrammetric techniques-Nea Paphos case study. Journal of Archaeological Science: Reports, 53, 104353.

Patel, S., Chintanadilok, J., Hall-Scharf, B., Zhuang, Y., Strickland, J., & Singh, A. (2024). WebODM: An Open-Source Alternative to Commercial Image Stitching Software for Uncrewed Aerial Systems: AE593, 2/2024. EDIS, 2024(1).

Pell, T., Li, J. Y., & Joyce, K. E. (2022). Demystifying the differences between structure-from-Motion Software packages for pre-processing drone data. Drones, 6(1), 24.

Przybilla, H. J., Bäumker, M., Luhmann, T., Hastedt, H., & Eilers, M. (2020). Interaction between direct georeferencing, control point configuration and camera self-calibration for RTK-based UAV photogrammetry. The International Archives of the Photogrammetry, Remote Sensing and Spatial Information Sciences, 43, 485-492.

Rupnik, E., Nex, F. & Remondino, F., (2013). Automatic orientation of large blocks of oblique images. ISPRS - International Archives of the Photogrammetry, Remote Sensing and Spatial Information Sciences.

Shen, S. “Accurate Multiple View 3D Reconstruction Using Patch-Based Stereo for Large-Scale Scenes.” IEEE Transactions on Image Processing 22, no. 5 (May 2013): 1901–14.

da Silva, T.v.d.W.; Gomes Pereira, L.; Oliveira, B.R.F. Assessing Geometric and Radiometric Accuracy of DJI P4 MS Imagery Processed with Agisoft Metashape for Shrubland Mapping. Remote Sens. 2024, 16, 4633.

Silva, L. Dias, F., Assis, V. C., Pinto, C. & Rangel, F. (2022). Validation of the positional accuracy of products resulting from the digital processing of UAV images. Brazilian Journal of Agricultural and Environmental Engineering, v. 26, n. 8, 624-630.

Triggs, B., McLauchlan, P. F., Hartley, R. I., & Fitzgibbon, A. W. (1999, September). Bundle adjustment—a modern synthesis. In International workshop on vision algorithms (pp. 298-372). Berlin, Heidelberg: Springer Berlin Heidelberg.

Vacca, G. (2020). WEB open drone map (WebODM) a software open source to photogrammetry process. In Fig Working Week 2020. Smart surveyors for land and water management.

Vivar-Vivar, E.D.; Pompa-García, M.; Martínez-Rivas, J.A.; Mora-Tembre, L.A. UAV-based Characterization of Tree-Attributes and Multispectral Indices in an Uneven-Aged Mixed Conifer-Broadleaf Forest. Remote Sens. 2022, 14, 2775.

Vong, A.; Matos-Carvalho, J.P.; Toffanin, P.; Pedro, D.; Azevedo, F.; Moutinho, F.; Garcia, N.C.; Mora, A. How to Build a 2D and 3D Aerial Multispectral Map?—All Steps Deeply Explained. Remote Sens. 2021, 13, 3227.

Thank you for your attention

Faculty of Geodesy and Cartography
Warsaw University of Technology

Open-Source vs. Commercial Photogrammetry: Comparing Accuracy and Efficiency of OpenDroneMap and Agisoft Metashape

Adam Kostrzewa, Anna Płatek-Żak, Przemysław Banat, Łukasz Wilk

EuroCOW - EUROPEAN WORKSHOP ON CALIBRATION AND ORIENTATION IN REMOTE SENSING
16.06.2025